Rare Metal Materials and Engineering
Volume 51, Issue 1, January 2022
Available online at www.rmme.ac.cn

Science Press

Cite this article as: Dong Xiongbo, Guo Yongchun, Li Jianping, et al. Effect of Ultrasonic Vibration on Solidification Microstructure in Near-Eutectic Al-Si Piston Alloy[J]. Rare Metal Materials and Engineering, 2022, 51(01): 11-17.

ARTICLE

Effect of Ultrasonic Vibration on Solidification Microstructure in Near-Eutectic Al-Si Piston Alloy

Dong Xiongbo[1], Guo Yongchun[1], Li Jianping[1], Xia Feng[1], Ma Zhijun[1], Yang Wei[1], Wang Jianli[1], Xu Tao[2], Liang Minxian[1]

[1] School of Materials Science and Chemical Engineering, Xi'an Technological University, Xi'an 710021, China; [2] Xi'an Comboo New Materials Technology Co., Ltd, Xi'an 710117, China

Abstract: The effect of ultrasonic vibration (USV) on solidification microstructure of Al-11.5Si-4Cu-2Ni-1Mg-0.45Fe (wt%) piston alloy was investigated. Results show that the significant refinement and morphology transformation from strip into compact polygon can be observed for the primary Si in the alloys produced by USV. The enhanced heterogeneous nucleation and shortened growth time caused by the large undercooling which is triggered by cavitation are responsible for the refinement of primary Si. The morphology of eutectic Si gradually develops from long plate into a short plate structure with increasing the ultrasonic power. Meanwhile, the morphology of α-Al_5FeSi phases changes from coarsening block shape to half circle. The morphology evolution and refinement of eutectic Si as well as intermetallic particles are mainly due to the fragmentation of solid crystals, homogeneous solute distribution field and temperature field, and shortened eutectic growth time caused by cavitation.

Key words: Al-Si alloys; ultrasonic vibration; microstructure; nucleation

Cast near-eutectic Al-Si alloys are widely used in automotive applications, especially in the piston industry due to their low thermal expansion, high strength, and high fatigue resistance at elevated temperatures[1-3]. As the heart of the engine, the working load of the piston is increased with the development of the engine towards high thermal efficiency, low emission, and lightweight[4]. However, under conventional casting conditions, the near-eutectic Al-Si piston alloy is prone to coarse microstructure, leading to the decrease in mechanical properties, especially in fatigue strength. A fine microstructure can improve the tensile strength of alloys, resulting in better mechanical properties[5,6].

Microstructure refinement has been successfully applied by modifier addition[7-10], melt overheating[11], rapid solidification[12], and ultrasonic vibration (USV)[13]. Among the various techniques, USV treatment has the refinement effect for silicon phase without changing the original composition of the alloys. Moreover, no pollution, simple equipment, convenient operation, and other advantages can be achieved through ultrasonic treatment. Sha et al[14] showed that USV treatment applied at the liquidus temperature on Al-20Si-2Cu-1Ni-0.7Fe-1.05Co alloys can not only refine the primary Si phase and reduce the precipitation of primary Si, but also decrease the size of Fe-containing compounds. Kotadia et al[15] reported that ultrasonic melting treatment results in significant refinement and better dispersion of primary Si particles. A lot of researches have been made about the effects of ultrasonic melt treatment on microstructure of near-eutectic Al-Si piston. However, few studies focused on the introduction of USV into the full solidification process of near-eutectic Al-Si piston alloy.

In this research, the effect of USV in full solidification process of Al-11.5Si-4Cu-2Ni-1Mg-0.45Fe alloy melt was investigated to clarify the role of USV in the microstructural evolution. Subsequently, the morphological transformation mechanism was also discussed based on the experiment results.

Received date: January 22, 2021
Foundation item: Shaanxi Provincial Scientific and Technological Research Project (S2018-YF-ZDLGY-0070); Shaanxi Creative Talents Promotion Plan-Technological Innovation Team (2017KCT-05)
Corresponding author: Li Jianping, Ph. D., Professor, School of Materials Science and Chemical Engineering, Xi'an Technological University, Xi'an 710021, P. R. China, Tel: 0086-29-86173324, E-mail: lijianping@xatu.edu.cn

1 Experiment

Industrial pure aluminum (99.9wt%), industrial pure magnesium (99.9wt%), crystalline silicon (98wt%), master alloys of Al-50Cu, Al-10Ni, Al-20Fe, and Al-10Mn, and La-Ce mixed rare earth alloy were used to prepare the Al-11.5Si-4Cu-2Ni-1Mg-0.45Fe piston alloy. All the element composition is expressed in mass ratio. For each experiment, the alloy of about 2 kg (approximate 0.8 L) was melted at 700 °C in a clay-bonded graphite crucible (diameter of 130 mm, height of 180 mm) by a high-frequency induction furnace of 50 kW. The melt temperature was monitored by a K-type thermocouple positioned at the melt next to the sonotrode. The melt was modified by P-salt and 0.35wt% La-Ce mixed rare earth alloy at 750 °C. Then, the melt was isothermally held at 750 °C for 20 min for complete homogenization. Subsequently, the alloy of about 200 g was poured into a pre-heated (500 °C) stainless steel specimen cup. The USV at frequency of 19 kHz was conducted using a titanium horn immersed at the place of 2 cm below the top melt surface, and then it was maintained throughout the solidification process until the melt was cooled down to 680 °C. In order to reduce the chill effect of cold horn, the titanium horn was preheated to 300 °C. The power of the ultrasounds was set as 0, 900, 1500, 2400, and 3000 W. The thermal analysis was conducted below the stainless steel specimen cup to examine the solidification status. Fig.1 shows the location of the thermocouple and ultrasonic horn in a stain steel specimen cup. Each cooling curve was recorded more than three times to ensure the accuracy of the tests.

The solidified alloy ingot specimens were symmetrically cut at the vibration point. Then a quarter of section piece (15 mm×15 mm×20 mm) was taken as the metallographic specimen. These specimens were polished by PG-2D polishing machine with a water-soluble diamond of 2.5 μm in size, and then etched by 0.5vol% HF for 30 s. The microstructure was observed by optical microscope (OM) and scanning electron microscope (SEM). Also, the quantitative metallography was conducted by Image-Pro Plus 6.0 software.

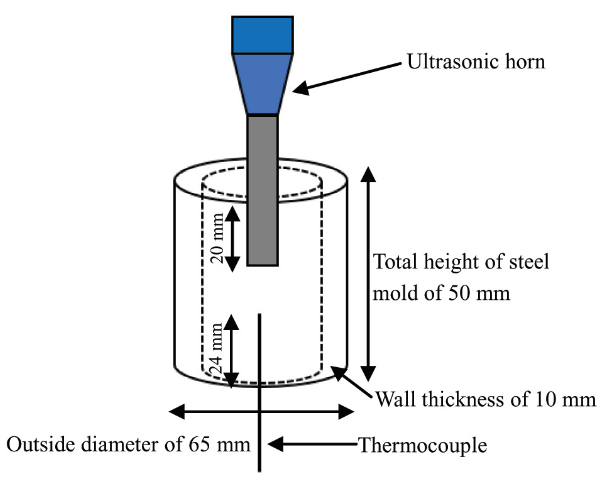

Fig.1 Schematic diagram of USV equipment and mold size

The average size, area fraction, and perimeter of primary Si were calculated in more than 15 optical fields (200×) to ensure the reproducibility. The length and width of 50 eutectic Si phases were calculated to investigate the effect of USV on eutectic Si. The diameter and shape factor were introduced to describe the size and morphology of the primary Si. The average primary Si size (D) and roundness (F) could be obtained by Eq.(1) and Eq.(2), respectively:

$$D = 2\sqrt{\frac{A}{\pi}} \tag{1}$$

$$F = \frac{4\pi A}{P^2} \tag{2}$$

where A and P are the area and perimeter of the primary Si, respectively.

2 Results

2.1 Effect of USV on Si phase

Fig. 2 represents the overall microstructure and eutectic morphologies of the Al-11.5Si-4Cu-2Ni-1Mg-0.45Fe piston alloys produced by USV at different powers. Dark gray phases are Si (faceted block primary Si and long plate eutectic Si) and the white microstructure is α-Al phase. A small amount of elongated primary Si can be observed in the alloy produced without USV (Fig.2a). Primary Si formed by USV has either compact polygonal or block shape and is uniformly distributed in the matrix, especially in the ones treated at high ultrasonic powers (dark gray phase in Fig.2b~2f). Moreover, the amount of relatively abundant primary Si is increased with increasing the ultrasonic power, which indicates the prolific nucleation of primary Si caused by cavitation. The eutectic Si with long plate morphology, which is the characteristic of untreated alloy (Fig. 2f), is transformed into a short plate structure with rounded edges and compact polygon after USV treatment at 3000 W, as shown in Fig.2j.

The size and roundness of the primary Si at different USV powers were quantitatively measured and the results are shown in Fig. 3a and 3b. It should be noted that with increasing the USV power, the average size of the primary Si is decreased. The roundness of primary Si tends to increase with increasing the USV power, showing a broader peak of frequency with larger USV power. It is clear that the size of primary Si is firstly decreased with USV power of 0~2400 W and then increased with USV power of 2400~3000 W, as shown in Fig.3c. This is mainly due to the thermal effect from ultrasonication which reduces the cooling rate. Fig.3d shows the length and width of eutectic Si in the alloy treated at different USV powers. It is clear that with increasing the USV power, the length of eutectic Si is reduced and the width is increased. For the alloy produced without USV, the average length and average width of eutectic Si are 18.6 and 0.92 μm, respectively. The best morphology of eutectic Si can be obtained in the alloy treated at USV power of 3000 W: the average length and average width of this eutectic Si are approximately 7.8 and 1.72 μm, respectively.

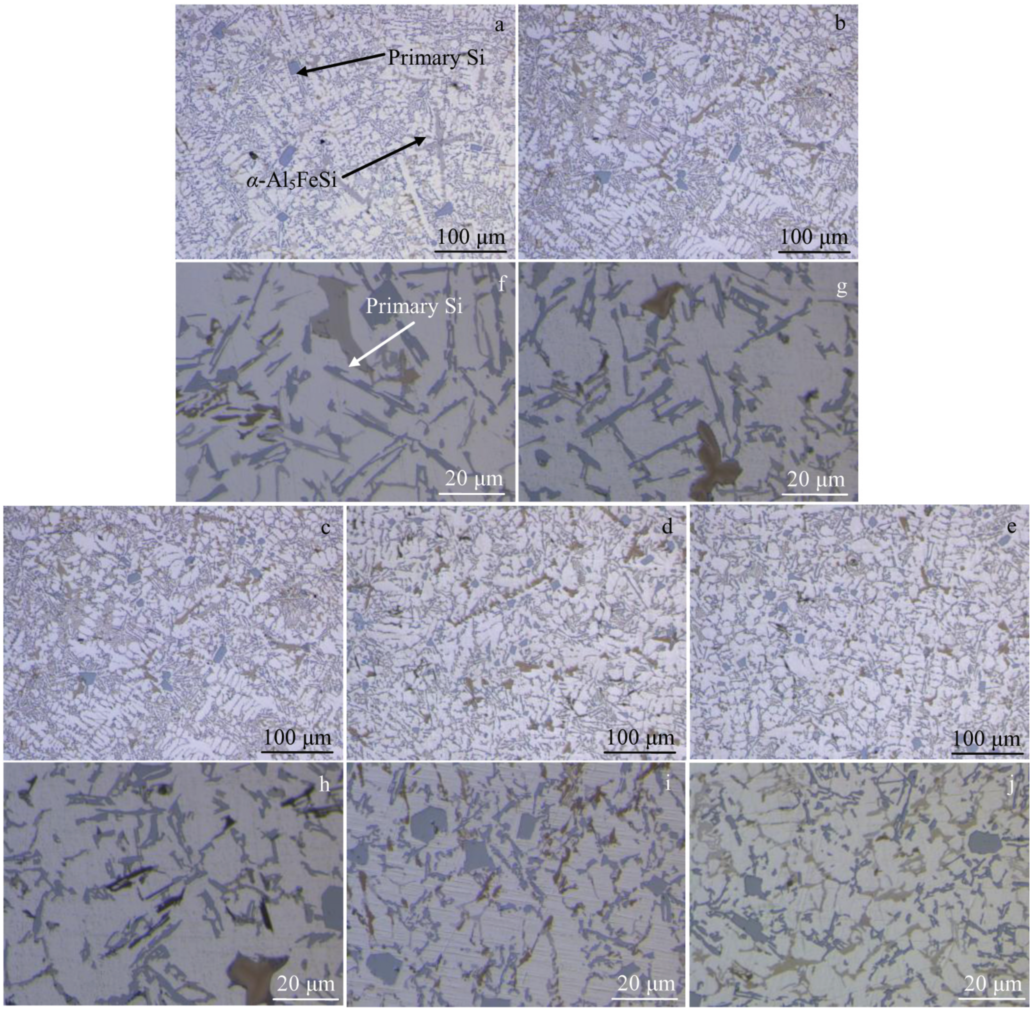

Fig.2 Microstructures of Al-11.5Si-4Cu-2Ni-1Mg-0.45Fe piston alloys at low (a~e) and high (f~j) magnifications treated at different USV powers: (a, f) 0 W, (b, g) 900 W, (c, h) 1500 W, (d, i) 2400 W, and (e, j) 3000 W

2.2 Effect of USV on intermetallics

Fig.4 shows SEM-EDS results and X-ray diffraction (XRD) patterns of the alloys treated by USV at different powers. It is clear that all alloys contain α-Al_5FeSi, δ-Al_3CuNi, and Q-$Al_5Cu_2Mg_8Si_6$ phases apart from α-Al and Si phases. It is also noteworthy that ultrasonication cannot modify the type of intermetallics. The chemical composition of the intermetallics was analyzed by energy dispersive spectroscope (EDS) and identified through the comparison with the results in Ref.[16], as shown in Table 1. As shown in Fig. 4a~4e, α-Al_5FeSi phase is the block shape in light gray; δ-Al_3CuNi phase is the shape of fish-bone in white; Q-$Al_5Cu_2Mg_8Si_6$ phase is the block shape in dark gray. Two groups of secondary phases, namely Si and aluminides, can also be distinguished by EDS element mapping, as shown in Fig 4g and 4h. The growth morphology of α-Al_5FeSi phase shows a distinct evolution from block shape (Fig. 4a~4c) to half circle with compact polygon (Fig. 4d and 4e) under ultrasonic exposure. Ultrasonication can refine the δ-Al_3CuNi phase rather than the coarse fish-bone-shaped morphology obtained through the conventional solidification route.

Fig. 5a and 5b show the area distribution of the α-Al_5FeSi and δ-Al_3CuNi phases in the USV treated alloys. It is clear that with increasing the ultrasonic power, the average areas of the α-Al_5FeSi and δ-Al_3CuNi phases are decreased with a sharp peak of frequency. Sha et al[14] reported that the Fe-containing phase with small size and small aspect ratio is beneficial to mechanical property. The δ-Al_3CuNi phase of small size is recognized as the most effective phase in improving the elevated-temperature properties of Al-Si piston alloys[17]. Thus, this morphological transformation of α-Al_5FeSi and δ-Al_3CuNi phases after USV treatment is conducive to the improvement of mechanical properties.

3 Discussion

The above results show a clear evidence of the effectiveness of ultrasonication in refining the microstructure. The microstructure refinement caused by ultrasound is mainly attributed to the cavitation effect and acoustic streaming effect in the melt, and the cavitation effect plays the more important

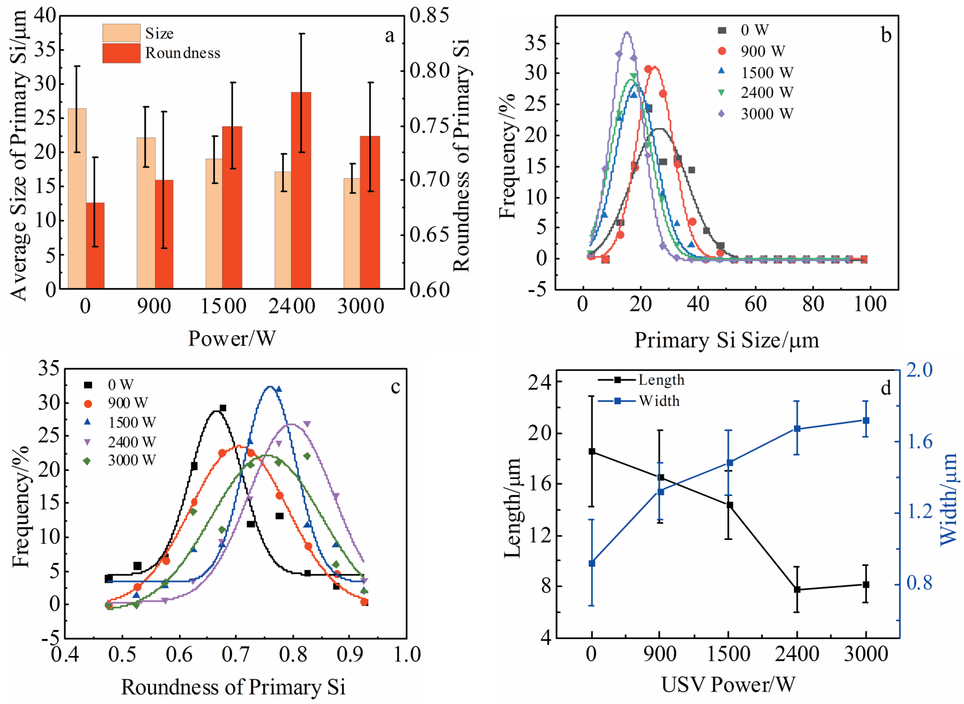

Fig.3 Average size and roundness of primary Si (a); size distribution of primary Si (b); roundness distribution of primary Si (c); length and width of eutectic Si (d)

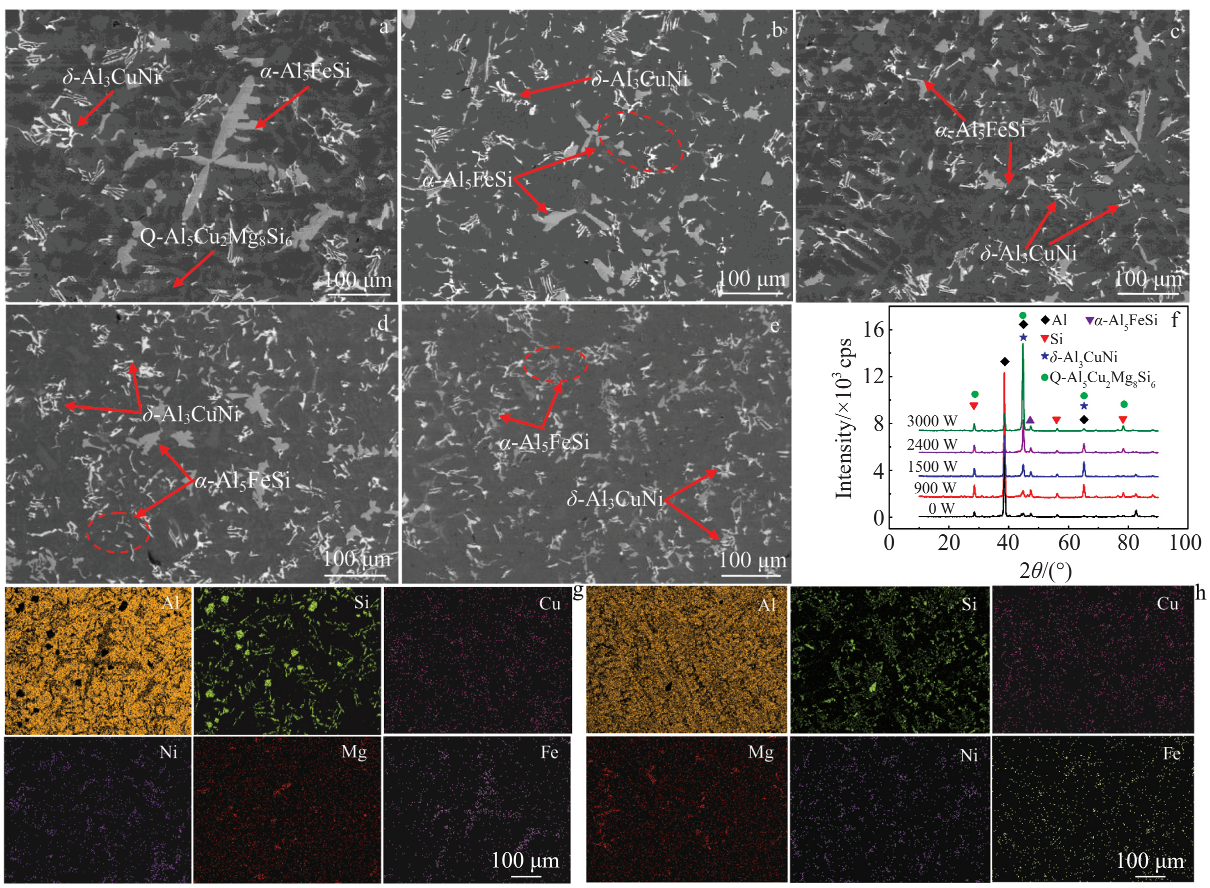

Fig.4 SEM images (a~e), XRD patterns (f) and EDS element mapping results of Fig.4a (g) and Fig.4e (h) of Al-11.5Si-4Cu-2Ni-1Mg-0.45Fe piston alloys treated at different USV powers: (a) 0 W, (b) 900 W, (c) 1500 W, (d) 2400 W, and (e) 3000 W

Table 1 EDS results of intermetallics observed in Al-11.5Si-4Cu-2Ni-1Mg-0.45Fe piston alloy without USV (wt%)

Phase	Al	Si	Cu	Ni	Mg	Mn	Fe
Q-$Al_5Cu_2Mg_8Si_6$	51.16	20.31	10.88	1.63	16.02	-	-
δ-Al_3CuNi	51.84	1.99	20.95	23.31	-	1.91	-
α-Al_5FeSi	66.17	12.76	0.49	4.51	-	7.49	8.58

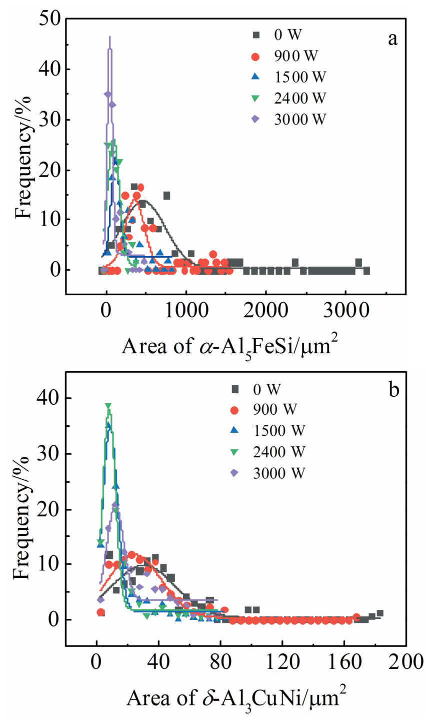

Fig.5 Area distributions of α-Al_5FeSi (a) and δ-Al_3CuNi (b) phases in Al-11.5Si-4Cu-2Ni-1Mg-0.45Fe piston alloys after USV treatment at different powers

role[18]. The difference in microstructure morphology, size, and distribution of alloys treated at different powers can also be attributed to the cavitation effect which produces a large number of tiny bubbles in the melt, namely cavitation bubbles. The relationship between the critical radius of cavitation bubble and the ultrasound pressure intensity can be expressed as follows:

$$R_{min}^3 + \frac{2\sigma}{P_0} R_{min}^2 - \frac{32\sigma^3}{27(P_m - P_0)} = 0 \tag{3}$$

where R_{min} is the critical nucleus radius of cavitation bubble under a certain ultrasound pressure; P_m is the ultrasonic sound pressure; P_0 is a constant; σ is the surface tension of the melt. Therefore, the larger the P_m generated by the ultrasonic wave, the smaller the R_{min} of the cavitation bubble. This phenomenon causes an increase in the number of cavitation bubbles. Thus, the morphology and size of final microstructure depend on the cavitation intensity and the number of cavitation bubbles at different ultrasonic powers which directly determine the number of solidified nuclei.

The refinement mechanism of primary Si can be divided into two stages: (1) pouring temperature-liquidus temperature; (2) below liquidus temperature. Between the pouring temperature and liquidus temperature, the refinement mechanism of primary Si is cavitation-enhanced heterogeneous nucleation, which is reflected in the cooling curves (Fig.6). The non-wetting impurity particles such as $MgAl_2O_4$ and Al_2O_3 particles can be wetted by ultrasound, which becomes an effective nucleation base of primary Si. Jung et al[19] reported that the ultrasonic melt treatment can activate the non-wetting $MgAl_2O_4$ particles and refine the AlP particles to improve the nucleating potency of primary Si. Below the liquidus temperature T_L, primary Si forms in this stage. Collapsing cavitation bubble produces shock waves which can shatter the coarsening of primary Si to ameliorate the morphology of primary Si. Eskin et al[20] reported that the collapsing cavitation bubble produces a shock wave of 100 MPa and a microjet of 100 m·s^{-1}. The existence of these two mechanisms is responsible for the refinement of primary Si after USV treatment. T_{nu} is the nucleation temperature of primary Si, T_{eu} is the eutectic reaction temperature, and t_{eu} is the eutectic reaction time.

To better understand the mechanism of microstructure refinement after USV treatment, the cooling curve of each specimen was obtained to reflect the nucleation and growth behavior of Si phase during solidification. Guo et al[21] proposed a new data processing method of characteristic value collected from the solidification cooling curves. The solidification parameters can be detected from Fig. 6a to reflect some important solidification events, as shown in Table 2. It is shown that with increasing the ultrasonic power, the

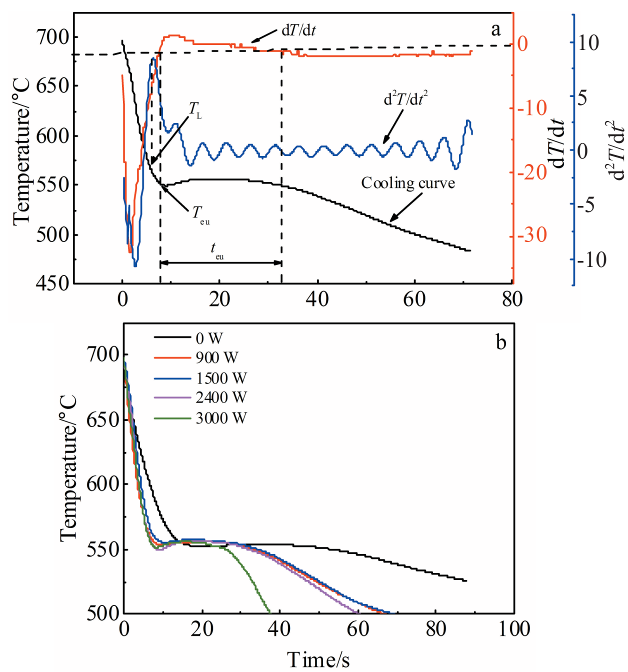

Fig.6 Cooling curve and solidification parameters of Al-Si piston alloy (a); cooling curves of Al-11.5Si-4Cu-2Ni-1Mg-0.45Fe piston alloys after USV treatment at different powers (b)

nucleation temperature of primary Si and eutectic Si is decreased. Wang et al[22] reported the similar results for Al-8wt% Si hypoeutectic alloy. The nucleation temperature of primary Si treated by USV at 3000 W decreases by 3.15% compared with that of the alloy produced without USV. This large effective nucleation undercooling can promote the heterogeneous nucleation in the available insoluble substrates such as oxides and other inclusions. Fig. 6b also shows the increased eutectic recalescence after USV treatment, which is attributed to the acoustic streaming effect. The eutectic recalescence occurs when the released latent heat for nucleation is higher than the heat extraction. Thus, the latent heat overcomes the heat extraction and then the temperature increases. This high eutectic recalescence can provide more active nucleation sites. Moreover, the cooling rates are increased with increasing the USV power until 2400 W, as shown in Table 2, which indicates that the growth time of primary Si is decreased during USV treatment. Therefore, the refinement of primary Si may be attributed to the enhanced heterogeneous nucleation and the decrease of growth time of primary Si.

The refinement mechanism of eutectic Si and intermetallics should be the same because they are formed in the stage of eutectic reaction. Under the experiment conditions in this research, the theory proposed by Zhang et al[23] seems to be a viable explanation for the modification of eutectic Si and intermetallics. It is reported that the fracture of Si plates causes the Si modification under ultrasonic exposure, because the shear stress applied on the Si particle caused by the collapse of cavitation bubbles is higher than the shear strength. Tzanakis[24] also reported that the fragmentation of solid crystals in cavitating liquids occurs through a fatigue-like mechanism triggered by oscillating bubbles and alternating acoustic flows. The similar mechanism can also explain the refinement of intermetallics under USV treatment. Fig. 7 shows the refinement mechanism of eutectic Si and intermetallics under USV treatment. The cavitation effect and acoustic streaming effect caused by USV can make the solute distribution field and temperature field more homogenous at the front of the eutectic reaction interface, which inhibits the rapid growth of eutectic Si and intermetallics along a single direction, resulting in the refinement of particles. In addition, the microjet and acoustic streaming can enhance the liquid flow, promote the atom diffusion, and reduce the thickness of the diffusion layer. Thus, the smaller Si particles in the melt are more likely to continuously aggregate, resulting in larger

Table 2 Solidification parameters of Al-Si alloy under different USV powers

Power/W	T_{nu}/°C	T_{eu}/°C	t_{eu}/s	Cooling rate/°C·s^{-1}
0	578.2	554.3	36.5	9.92
900	569.2	553.2	21.0	19.35
1500	565.4	551.8	18.6	20.08
2400	562.8	551.3	17.6	21.05
3000	560.0	552.6	15.4	17.90

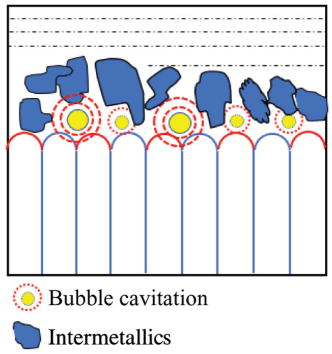

Fig.7 Mechanism of intermetallic refinement by USV

Si particles. When the Si particles contact with each other, they will automatically stick to each other, resulting in the increase in width of the eutectic Si. It is also clear that the eutectic reaction temperatures are almost identical for all specimens. Nevertheless, the eutectic growth time is decreased with increasing the ultrasonic power. These facts indicate that the shortened eutectic growth time plays a major role in the morphology changes under ultrasonic irradiation.

4 Conclusions

1) Ultrasonic vibration (USV) during solidification is an environmentally clean and efficient method which promotes the refinement of the primary Si, eutectic Si, and intermetallic phases.

2) USV promotes the change of elongated primary Si morphology into compact polygonal morphology. The size of primary Si depends on the ultrasonic power. The enhanced heterogeneous nucleation and decreased growth time under USV treatment result in the refinement of primary Si.

3) Eutectic Si with long plate morphology, which is the typical characteristic of conventional casting, changes into a short plate structure with rounded edges and compact polygon under ultrasonic exposure. The α-Al_5FeSi phase shows a similar change from the coarsening block shape into half circle morphology under USV treatment.

4) The fragmentation of solid crystals, homogeneous solute distribution field and temperature field, and shortened eutectic reaction time are responsible for the refinement of eutectic microstructure under USV treatment.

References

1 Li J H, Albu M, Hofer F *et al. Acta Materialia*[J], 2015, 83: 187

2 Han L N, Sui Y D, Wang Q D *et al. Journal of Alloys and Compounds*[J], 2017, 695: 1566

3 Li Bin, Yang Zhao, Yang Xuyue *et al. Rare Metal Materials and Engineering*[J], 2015, 44(11): 2858 (in Chinese)

4 Joyce M R, Styles C M, Reed P A S. *International Journal of Fatigue*[J], 2003, 25(9-11): 863

5 Chen Zhiqiang, Jia Jinyu, Hu Wenxin *et al. Rare Metal Materials and Engineering*[J], 2020, 49(10): 3388

6 Gall K, Horstemeyer M, Mcdowell D L *et al*. *Mechanics of Materials*[J], 2000, 32(5): 277
7 Li J H, Hage F S, Liu X F *et al*. *Scientific Reports*[J], 2016, 6: 25 244
8 Liang S M, Schmid-Fetzer R. *Acta Materialia*[J], 2014, 72: 41
9 Fatahalla N, Hafiz M, Abdulkhalek M. *Journal of Materials Science*[J], 1999, 34(14): 3555
10 Wang S, Fu M, Li X Z *et al*. *Journal of Materials Processing Technology*[J], 2018, 255: 105
11 Xu C L, Jiang Q C. *Materials Science and Engineering A*[J], 2006, 437(2): 451
12 Xu C L, Wang H Y, Qiu F *et al*. *Materials Science and Engineering A*[J], 2006, 417(1-2): 275
13 Jung J G, Lee J M, Cho Y H *et al*. *Journal of Alloys and Compounds*[J], 2017, 693: 201
14 Sha M, Wu S S, Wan L *et al*. *Materials Science and Engineering A*[J], 2012, 554: 142
15 Kotadia H R, Das A. *Journal of Alloys and Compounds*[J], 2015, 620: 1
16 Belov N A, Eskin D G, Avxentieva N N. *Acta Materialia*[J], 2005, 53(17): 4709
17 Li Y G, Yang Y, Wu Y Y *et al*. *Materials Science and Engineering A*[J], 2010, 527(26): 7132
18 Xue Hansong, Chen Yangyang, Huang Jie *et al*. *Rare Metal Materials and Engineering*[J], 2019, 48(7): 2049
19 Jung J G, Ahn T Y, Cho Y H *et al*. *Acta Materialia*[J], 2018, 144: 31
20 Eskin G I. *Ultrasonics Sonochemistry*[J], 2001, 8(3): 319
21 Guo Yongchun, Dong Xiongbo, Li Jianping *et al*. *Chinese Journal of Rare Metals*[J], 2018, 42(7): 713 (in Chinese)
22 Wang J Y, Wang B J, Huang L F. *Materials Science and Technology*[J], 2017, 33(11): 1235
23 Zhang S L, Zhao Y T, Cheng X N *et al*. *Journal of Alloys and Compounds*[J], 2009, 470: 168
24 Tzanakis I, Lebon G S B, Eskin D G *et al*. *Materials and Design*[J], 2016, 90: 979

超声振动对近共晶 Al-Si 活塞合金凝固组织的影响

董雄博[1]，郭永春[1]，李建平[1]，夏　峰[1]，马志军[1]，杨　伟[1]，王建利[1]，胥　涛[2]，梁民宪[1]

(1. 西安工业大学　材料与化工学院，陕西　西安　710021)

(2. 西安康博新材料科技有限公司，陕西　西安　710117)

摘　要：研究了超声振动对 Al-11.5Si-4Cu-2Ni-1Mg-0.45Fe 合金凝固组织的影响。结果表明，经超声振动的合金中，初生硅形貌由长条状转变为多边形状，并得到了显著细化。其中空化效应产生的大过冷度引起的异质形核和生长时间缩短是初生硅细化的主要原因。随着超声功率的增加，初生硅由长条状转变为短棒状，α-Al_5FeSi 相由块状转变为半圆形态。共晶硅和金属间化合物形态的演变和细化主要是由空化效应引起的固体破碎、均匀的溶质分布、均匀的温度场及共晶生长时间的缩短造成的。

关键词：Al-Si 合金；超声振动；组织；形核

作者简介：董雄博，男，1991 年生，硕士，西安工业大学材料与化工学院，陕西　西安　710021，电话：029-86173324，E-mail：xbdong_0121@163.com